International Journal of Mass Spectrometry 301 (2011) 74–83

Contents lists available at ScienceDirect

International Journal of Mass Spectrometry

journal homepage: www.elsevier.com/locate/ijms

The effect of ion trap temperature on the dissociation of peptide ions in a quadrupole ion trap

April L. Jue, Alawee H. Racine, Gary L. Glish*

Department of Chemistry, University of North Carolina, Chapel Hill, NC 27599, United States

ARTICLE INFO

Article history:
Received 10 May 2010
Received in revised form 29 June 2010
Accepted 30 June 2010
Available online 15 July 2010

Keywords:
Quadrupole ion trap
Peptide sequencing
Collision-induced dissociation
Tandem mass spectrometry
Internal energy

ABSTRACT

Thermally-assisted collision-induced dissociation can substantially increase the amount of dissociation in quadrupole ion trap mass spectrometer experiments. The experiments discussed here were performed to assess the effect on dissociation pathways as the bath gas temperature is increased in thermally-assisted collision-induced dissociation (TA-CID) experiments. Double resonance experiments in which a product ion was ejected during collision-induced dissociation of the parent ion provided data to asses competitive versus consecutive dissociation pathways. Consecutive dissociation pathways are indicated when lower mass product ions decrease in intensity when a higher mass product ion is ejected during CID. For the peptide ions studied, those that dissociate to give predominately N-terminal product ions show increased consecutive dissociation with increased temperature during TA-CID. For peptide ions that dissociate via formation of C-terminal product ions, competitive dissociation pathways were more prevalent and increasing the temperature had much less effect. N-terminal product ions consecutively dissociate to smaller N-terminal ions whereas C-terminal product ions dissociate to internal fragments.

1. Introduction

Quadrupole ion trap mass spectrometers (QITMS) are well known for their high efficiency for tandem mass spectrometry (MS/MS) experiments. Over the years QITMS have become one of the most commonly used instruments for peptide sequencing. The multistage MS/MS (MS^n) capabilities [1–3] of the QITMS offer an important advantage over other mass spectrometers for peptide ion dissociation pathway analysis via collision-induced dissociation (CID). Parent ions are resonantly excited, which increases their kinetic energy to effect CID. They collide with the bath gas and ion kinetic energy is converted to ion internal energy. As long as the ion reaches the critical energy of dissociation before the ion's kinetic energy exceeds the trapping well and the ion is resonantly ejected, the parent ion can dissociate into product ions. A balance must exist between resonance excitation and resonance ejection as an ion's motion must be small enough to remain in the ion trap but increased enough so that the kinetic energy to internal energy conversion can induce ion dissociation [4]. Product ions that are formed are not in resonance with the applied voltage and thus undergo little further activation and in fact lose internal energy from collisions with the bath gas [5–7]. A result of this collisional activation process is that while the overall efficiency of dissociation of the parent ion is typically high, the number of product ions of different mass-to-charge that are formed is often limited, especially in contrast to beam instruments such as triple quadrupoles or quadrupole/time-of-flight instruments. This can be good for the study of dissociation pathways, but can limit the structural information obtained from unknowns. MS^n experiments can help improve peptide identification [8].

A product ion can be formed by one of two general processes: either directly from the parent ion or via sequential (consecutive) dissociation. Consecutive dissociation is a process in which a product ion, P_2, in the MS/MS spectrum is formed from another product ion, P_1, which has been formed with excess internal energy. This is in contrast to competitive dissociation that occurs when product ion P_2 is formed directly from the parent ion, as is product ion P_1. It has been well documented that b_n ions are prominent in most peptide CID spectra and readily fragment to form a_n ions (corresponding to the loss of CO from the b ion) and b_{n-1} ions [9]. Other studies have found that lower b_{n-1} ions arise from direct dissociation of b_n ions only 50% of the time [10].

A unique experiment which ion trapping instruments are capable of that further enhances the study of dissociation pathways is selective ejection of a specific product ion simultaneous with CID of the parent ion [11], a so-called "double resonance" experiment. The other product ions are not directly affected if they are not too near the mass-to-charge of the ion being ejected because they are not in resonance with either the voltage used to excite the parent ion or eject the specific product ion. However, intensities of

* Corresponding author. Tel.: +1 919 962 2303.
E-mail address: glish@unc.edu (G.L. Glish).

1387-3806/$ – see front matter © 2010 Elsevier B.V. All rights reserved.
doi:10.1016/j.ijms.2010.06.038

other product ions can be indirectly affected by the ejection of the selected product ion if the ejected product ion is an intermediate in the dissociation pathway [11]. Thus, a change in intensity of a product ion not in resonance provides information about the dissociation pathway. In fact, double resonance experiments have verified the existence of unobserved intermediate ions in the formation of product ions [11]. Other experiments have shown that b_n-NH_3 and a_n-NH_3 ions are not consecutive dissociation products of b_n and a_n ions but instead result directly from the dissociation of the $[M+H-NH_3]^+$ ion [12].

Peptide fragmentation may be influenced by the basicity or acidity of the amino acids [13,14] or the nature of the cationizing species [15–18]. For example, enhanced cleavage occurs at aspartic acid residues [15,19,20] and protonated histidine [12,21] residues while the presence of proline has been found to specifically enhance N-terminal cleavage [22–25]. Additionally, it has been shown that the dissociation of analogs of the peptide YGGFL to the a_4 product ion depends on the nature of the fourth amino acid [10]. Though b_n ions have been found to favorably dissociate further to a_n and lower mass-to-charge b_n product ions, C-terminus fragmentation involves separate pathways for y_4, y_3 and y_2 ions [26]. Multiple-resonance CID was used to establish the low-energy sequential decomposition pathways of YGGFL [26]. The y ions in this peptide dissociated to form internal ions instead of the lower mass-to-charge y ions.

Statistical and theoretical techniques have also been used to analyze peptide ion fragmentation pathways. A kinetic model has been created for the purpose of evaluating the fragmentation process that simulates the low-energy collision-induced dissociation spectra of peptides dissociated in a quadrupole ion trap [27]. Additionally, the statistical test of equivalent pathways (STEP) analysis uses the ion abundance of product ions in two MS/MS spectra to calculate a ratio that can be used to determine whether a product ion has been formed competitively or consecutively [28].

In the QITMS the bath gas also affects fragmentation pathways [4,29–32]. The bath gas in the trapping volume serves two purposes. The primary purpose is to collisionally cool the ions' kinetic energy. Decreasing the kinetic energy of the ions focuses them toward the center of the trapping volume. This improves resolution and sensitivity [33]. In addition to the kinetic cooling, collisional cooling can also decrease the internal energy of an ion [6,7]. This can reduce the dissociation of ions in MS/MS experiments [31,34]. The second purpose of the bath gas is to serve as the target in CID. An ion's kinetic energy can be increased via resonance excitation and then can be converted to internal energy in a collision with the bath gas. This is just the opposite of collisional cooling. Several studies have shown that using heavier bath gases (such as argon) increases the amount of internal energy that is deposited in the parent ion leading to much more dissociation [4,29,30]. This is a result of more effective conversion of kinetic energy to internal energy with increasing mass of the target. It has been suggested that the observation of many low mass-to-charge ions in the MS/MS spectra indicate a propensity for consecutive dissociation when heavier bath gases are used [30].

Furthermore, the bath gas temperature can affect the appearance of the mass spectra by either determining the kinetics for the first-generation product ion cooling or by thermally activating the dissociation of first and subsequent generation product ions [31,32]. The extent to which the temperature of the bath gas is able to affect the dissociation pathways is largely dependent upon the difference in the ion's internal energy and the temperature of the bath gas.

Thermally-assisted collision-induced dissociation (TA-CID) can be used to access additional dissociation pathways that are inaccessible at ambient temperatures [35]. When the bath gas temperature is elevated, the parent ions have more initial internal energy as a result of effectively being in thermal equilibrium with the bath gas. With more initial internal energy the dissociation efficiency of the parent ion is increased under equivalent CID conditions used at ambient temperature, resulting in more structural information [35].

Clearly, peptide fragmentation pathways are complicated. Because the dissociation pathways that are observed depend upon the amount of internal energy in the parent ion and the rate of collisional cooling of the product ions, the type of product ions that are seen and the relative abundances of these product ions can be expected to vary when different bath gas temperatures are employed. It has already been shown that more product ions are observed when TA-CID is used [35]. However, it has not been studied how these product ions are formed, i.e., which dissociation pathways increase with changes in temperature. In this work, we analyze the changing competitive and consecutive dissociation pathways in three different peptides at three different bath gas temperatures. Understanding the dissociation pathways that are accessed by increasing the thermal energy may allow algorithms to be developed that would increase the confidence of identification similar to that obtained by doing multiple stages of mass spectrometry [8].

2. Experimental

2.1. Materials

Three peptides were chosen for analysis and used without further purification. YGGFL was obtained from Sigma. FLLVPLG was synthesized by Bayer Corp. LLFGYPVYV was synthesized in the Department of Biochemistry at the University of North Carolina at Chapel Hill. All three peptides were dissolved in 75/20/5 percent methanol/water/acetic acid to a concentration of 100 μM.

2.2. Mass spectrometry

Experiments were performed in a customized Finnigan quadrupole ion trap mass spectrometer with a custom nano-electrospray source. Helium was used as the bath gas and kept at a pressure 8.4×10^{-4} Torr. The ion trap electrodes were heated to 100 °C and 160 °C using a 1000-W stab-in bakeout heater as described previously [34]. Experiments were also performed at ambient temperature (30 °C). CID was performed at a parent ion q_z value of 0.25 and resonant excitation amplitudes of 140 mV, 280 mV and 580 mV for YGGFL, FLLVPLG and LLFGYPVYV, respectively.

Dissociation pathways were analyzed by double resonance experiments [10,11]. The parent ion of interest was isolated in the quadrupole ion trap and resonantly excited and dissociated to generate product ions. During the resonant excitation of the parent ion, one of the product ions was resonantly ejected. A stored waveform inverse Fourier transform (SWIFT) waveform was built that encompassed a narrow range of frequencies to eject the first-generation product ion during the parent ion dissociation event. This is called the "double resonance" spectrum. The double resonance spectrum was compared with one obtained in the normal operating mode, i.e., without resonantly ejecting any product ion. To determine the effect of the first-generation product ion ejection the intensity of a product ion in the double resonance spectrum was divided by the intensity of that same product ion in the CID spectrum and then multiplied by 100. This value was subtracted from 100 to yield the "percent decrease" for the product ion that resulted from the ejection event. Dissociation pathway trees were created at each temperature using the percent decreases of the product ions to outline how the product ions dissociated on the time-scale of the experiment to yield the final CID spectrum.

To correct for the possibility that the first-generation product ion dissociated before it was ejected, an MS^3 type experiment was performed. The first-generation product ion was isolated and then resonantly ejected at the voltage used in the double resonance experiment. The appearance of lower mass-to-charge product ions showed if the first-generation product ion dissociated during the ejection process. The ion intensities in this control experiment were subtracted from the resonance ejection spectrum. In a second experiment to assess the possibility of ejecting/exciting product ions near the product ion being resonantly ejected an MS^4 type experiment was performed. The first-generation product ion was isolated and then dissociated in a conventional MS^3. After the first-generation product ion was dissociated a spectrum was collected. Then the resonant ejection voltage used in the double resonance experiment was applied and another spectrum was collected. Product ions within a 15 mass-to-charge range on either side were monitored for decreases in intensity. Any relative signal intensity decrease (calculated from comparing these two control spectra) was added to the resonance ejection spectrum. This control experiment served to correct for the unintentional ejection of nearby product ions when resonance ejection was applied to the first-generation product ion.

3. Results and discussion

In Fig. 1a, the CID spectrum of YGGFL is shown. Fig. 1b is the double resonance spectrum where the first-generation product ion, b_4, has been resonantly ejected during CID of $[M+H]^+$. In Fig. 1b, the signal intensity of the a_4 product ion is greatly reduced when the b_4 product ion is ejected during CID of the $[M+H]^+$ ion. This indicates that most of the a_4 product ion observed in Fig. 1a is formed from the dissociation of protonated YGGFL to the b_4 product ion which consecutively dissociates to the a_4 product ion, as previously reported [10]. The signal intensity of the b_3 product ion is only slightly reduced when the b_4 product ion is ejected from the spectrum. Therefore, the b_3 product ion is not primarily formed from the consecutive dissociation of the b_4 product ion; it is formed directly from the protonated parent ion or by additional dissociation pathways that have not yet been characterized.

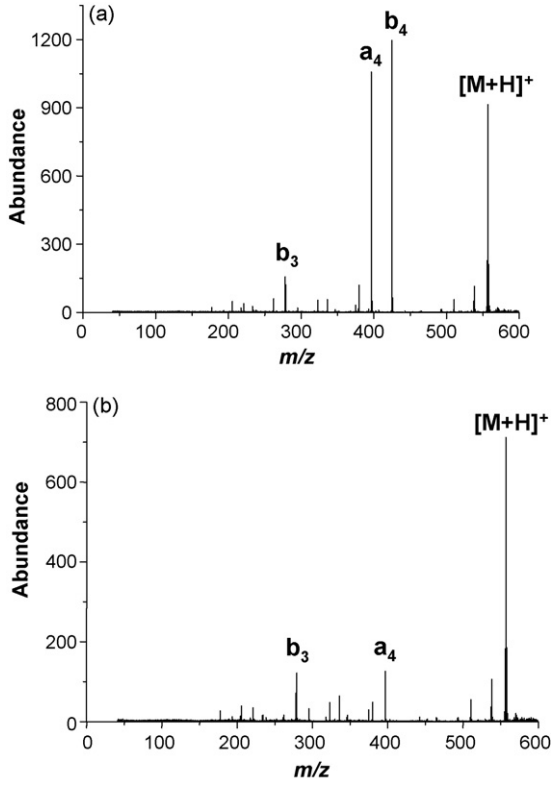

Fig. 1. YGGFL, 30 °C (a) CID of YGGFL (b) CID of YGGFL and simultaneous ejection of the b_4 product ion.

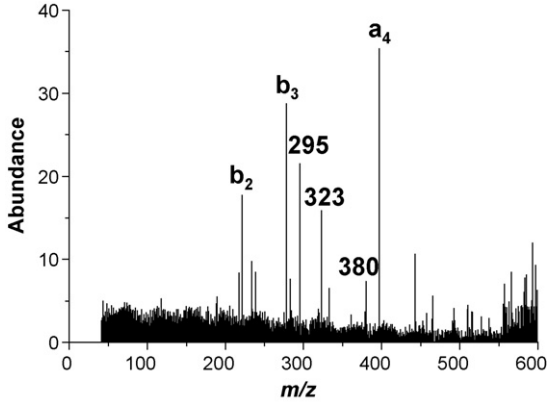

Fig. 2. YGGFL, 30 °C. First control experiment – ejection of the isolated b_4 product ion at 3000 mV.

Two control experiments were done for each double resonance experiment. The first control experiment corrects for the unintentional dissociation of the resonantly ejected product ion. Ideally, a resonantly ejected product ion should be completely ejected when a resonance excitation voltage is applied to the endcaps at the appropriate frequency. However, as can be seen in Fig. 2, when the isolated b_4 product ion is resonantly ejected using 3000 mV, a small amount dissociates before it can be ejected, leading to the lower mass-to-charge peaks observed in Fig. 2. This dissociation is corrected for by subtracting the signal intensity observed in Fig. 2 from the resonance ejection spectrum shown in Fig. 1b.

The second control experiment corrects for the ejection of other product ions near the product ion being resonantly ejected in the double resonance spectrum. In an MS^3 experiment, the b_4 product ion was isolated, and then dissociated (Fig. 3a) and then the double resonance ejection voltage was applied to ejected it (Fig. 3b). This allowed for correction of any decrease in signal intensity observed in the neighboring product ions that may have been caused by the ejection of the b_4 product ion. When the resonance ejection was performed at 3000 mV, the neighboring product ions were usually not affected. The MS^3 control experiment, however, also provided information about the potential dissociation pathways of the resonantly ejected ions. For example, the MS^3 spectrum shown in Fig. 3a indicates that b_4 dissociates to a_4, the most abundant product ion observed in this CID spectrum. Other product ions that are less abundant in the spectrum include the m/z 380, m/z 323, m/z 295 and b_3 ion. The ions at m/z 323 are the result of a rearrangement in which the C-terminal amino acid residue of the a_4 ion (F in this case) is transferred to the N-terminus followed by the loss of the third amino acid (G). The ions at m/z 295 are a result of loss of CO from 323 and m/z 380 is $[a_4\text{-}NH_3]^+$ [36]. When these same peaks are examined in the experimental resonance ejection spectrum (Fig. 1b), the a_4 signal intensity is found to decrease most drastically when b_4 is ejected. The other ions that are observed in the MS^3 spectrum (Fig. 3a) also decrease in Fig. 1b, though not to the same extent as the a_4 product ion.

When the bath gas temperature is elevated during CID experiments performed in the QITMS, the YGGFL product ion distribution changes (Table 1). As the temperature is increased from 30 °C to 160 °C the a_4/b_4 ratio increases. Previous studies have found that the a_4/b_4 ion intensity ratio is a good indicator of the parent ion

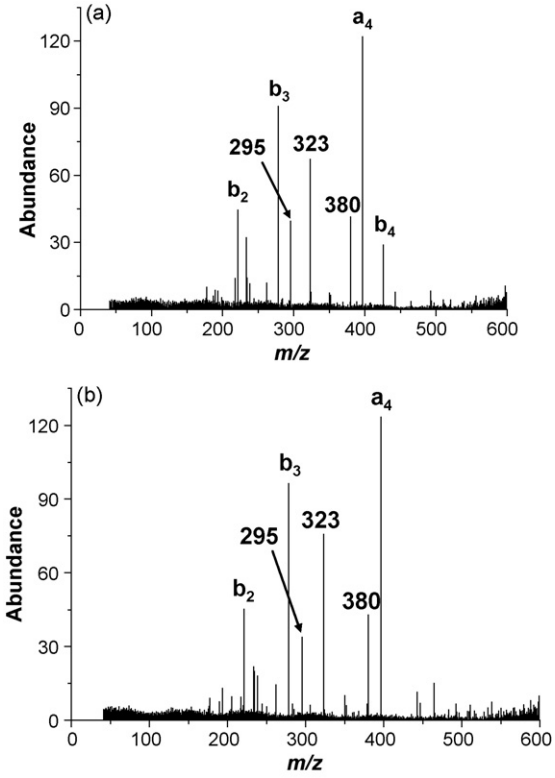

Fig. 3. YGGFL, 30 °C. Second control experiment. (a) CID of the first-generation b_4 product ion (MS^3). (b) Ejection of the b_4 product ion after MS^3.

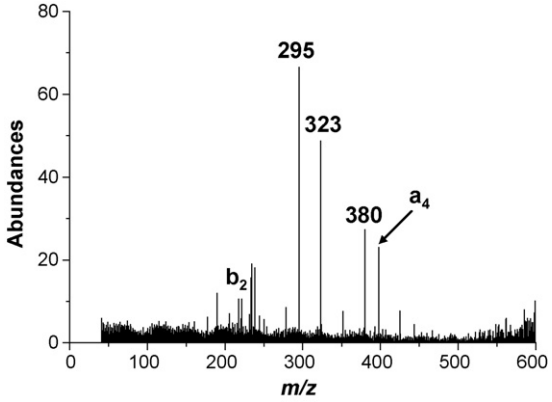

Fig. 4. YGGFL, 30 °C. Second control experiment – CID of the a_4 product ion (MS^3).

([M+H]$^+$) internal energy for YGGFL [37]. At higher temperatures, the parent ion has more internal energy and a higher a_4/b_4 ratio. The current results agreed with the previous findings. Table 1 also shows that the smaller b and a-type product ions increase in overall spectral abundance from 30 °C to 100 °C but decrease at 160 °C. This may be a direct result of the changing a_4/b_4 ratio. At 160 °C, there is significantly more a_4 product ion formed than b_4 product ion. Previous studies have found that the a_4 product ion tends to dissociate to *m/z* 380, *m/z* 323, and *m/z* 295 [36]. Table 1 shows that as more a_4 is formed, the *m/z* 380 and *m/z* 323 peak abundance increases. Hence, the decrease in lower b and a-type product ions may result from the fact that these pathways are less accessible as the a_4 ion relative abundance increases and favors the dissociation pathway to the *m/z* 380, *m/z* 323, and *m/z* 295 product ions. The MS^3 spectrum for the a_4 product ion (Fig. 4) also supports the dissociation of a_4 primarily to *m/z* 380, *m/z* 323, and *m/z* 295 product ions.

Table 1 provides preliminary support for the existence of differences in peptide dissociation pathways at different temperatures in the quadrupole ion trap. At 100 °C, all of the lower mass-to-charge product ions increase in abundance while at 160 °C only the *m/z* 380, *m/z* 323, and *m/z* 295 product ions continue to increase in abundance. It is unclear, however, from the data shown whether the lower mass-to-charge product ions are changing in abundance due to increased consecutive or competitive dissociation pathways.

To gain further insight into this matter, dissociation pathway trees that illustrate the observed dissociation pathways for the peptide at each temperature were generated. Generally, only product ions above a certain threshold intensity were analyzed (~50 absolute intensity or greater on the data system scale). Scheme 1a shows the dissociation pathway tree for YGGFL at 30 °C. At 30 °C, YGGFL is able to dissociate to one of four first-generation production ions, b_4, a_4, *m/z* 380, or b_3. Out of these four first-generation product ions, b_4 and a_4 further dissociate into second-stage product ions. Of the five second-stage product ions, only a_4 dissociates into third-stage product ions. Next to each arrow in the tree is a number that is the abundance of that pathway. The abundance of each pathway allows the origins of each product ion in the CID spectrum to be determined. When YGGFL dissociates into first-generation product ions, b_4 forms 93% of the first-generation product ion spectrum. The other product ions, a_4, *m/z* 380, and b_3, account for 4%, 0.8%, and 2.2% of the spectrum, respectively. However, the intensity of the b_4 ion observed in the MS/MS spectrum is not 93% because some of the b_4 ions can subsequently dissociate to lower mass product ions on the time-scale of the experiment. Instead of accounting for 93% of the first-generation product ion spectrum b_4 accounts for only about 52% of the product ions observed, 43% of the b_4 product ions dissociate to the a_4 product ion. Additionally, b_4 dissociates to the *m/z* 380 and b_3 product ions, albeit in much smaller proportions. The a_4 product ions are able to consecutively dissociate in a similar manner to the *m/z* 380, *m/z* 323, *m/z* 295, and b_3 product ions. The rest of the product ions shown in Scheme 1 as coming directly from the protonated YGGFL ([M+H]$^+$) may be direct dissociation or could be from consecutive dissociation of b_4 that occurs faster than the b_4 ion can be ejected in the double resonance experiment. Previous experiments determined that it is unlikely there is enough excess internal energy in the b_4 product ion to dissociate within the 50 μs it takes to eject it [10]. If it is assumed that these product ions come directly from the [M+H]$^+$, at 30 °C, Scheme 1a shows that 2.2% of the total 5.4% b_3 product ion intensity in the MS/MS spectrum is formed directly from the dissociation of YGGFL. The two-step consecutive dissociation pathways ([M+H]$^+ \rightarrow b_4 \rightarrow b_3$ and [M+H]$^+ \rightarrow a_4 \rightarrow b_3$) account for 1.0% of the total b_3 product ion, while the three-step consecutive dissocia-

Table 1
Relative abundances of the major YGGFL product ions at different temperatures.

Temperature (°C)	Product ion							
	b_4	a_4	*m/z* 380	*m/z* 323	*m/z* 295	b_3	b_2	a_2
30	48.1	38.9	3.8	1.9	0.6	5.4	1.2	0.2
100	29.7	44.4	5.4	3.6	1.1	11.2	4.3	0.5
160	26.5	53.4	6.9	3.8	1.1	6.9	1.4	0.2

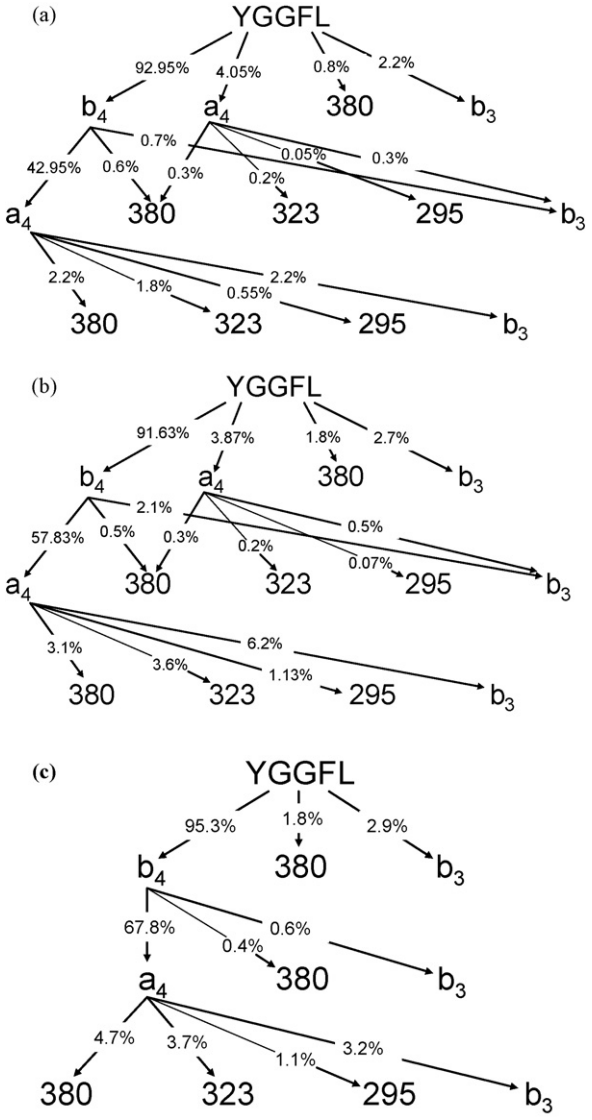

Scheme 1. Dissociation pathway trees depicting the dissociation pathways of YGGFL. Next to each arrow is a number displaying the abundance of that dissociation pathway. (a) 30 °C, (b) 100 °C, and (c) 160 °C.

tion pathway ($[M+H]^+ \rightarrow b_4 \rightarrow a_4 \rightarrow b_3$) accounts for the remaining 2.2% of the total b_3 product ion composition. The b_3 ion appears to be a terminal ion. This is probably because most b_3 ions do not undergo the usual loss of CO to form a_3 like other b_n ions [38]; however, because the overall intensity is low, it is possible that there is insufficient sensitivity to detect consecutive dissociation.

Scheme 1b and c shows the same dissociation pathway trees for YGGFL at 100 °C and 160 °C, respectively. These schemes show that both consecutive and competitive dissociation pathways are affected at elevated temperatures. Although the ions with lower mass-to-charge ratios generally have higher relative abundances at elevated temperatures, this does not necessarily always correlate with an increase in a dissociation pathway. Therefore, product ion formation trees at different temperatures were also created that traced the relative contribution of the dissociation pathways to the formation of a given product ion. For example, the 2.2% of the b_3 product ion formed directly from the parent ion at 30 °C accounts for 40.7% of the b_3 ion intensity in the MS/MS spectrum. This is obtained by dividing the 2.2 relative intensity of the $[M+H]^+ \rightarrow b_3$ pathway, by the total b_3 ion intensity of 5.4 (2.2 + 0.7 from $[M+H]^+ \rightarrow b_4 \rightarrow b_3$ + 0.3 from $[M+H]^+ \rightarrow a_4 \rightarrow b_3$ + 2.2 from

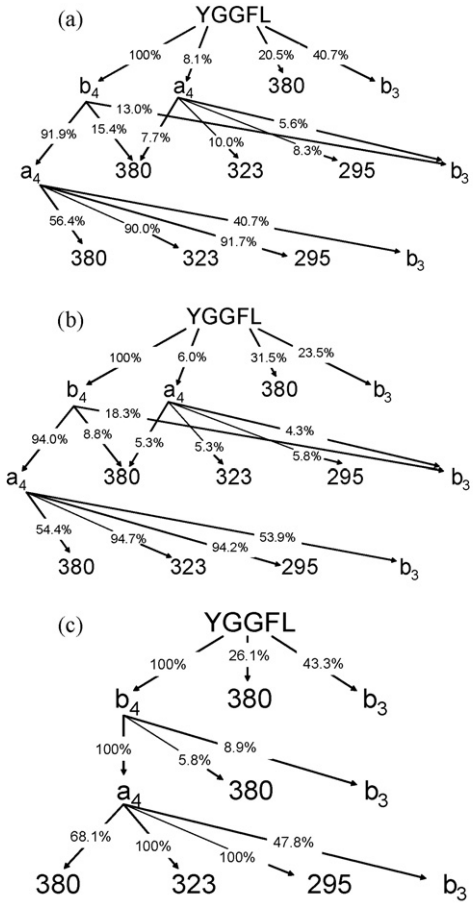

Scheme 2. Product ion formation pathway trees for YGGFL. Next to each arrow is the relative abundance of that that pathway contributing to the formation of that particular product ion. (a) 30 °C, (b) 100 °C, and (c) 160 °C.

$[M+H]^+ \rightarrow b_4 \rightarrow a_4 \rightarrow b_3$). Scheme 2a–c show the product ion formation pathways for YGGFL at 30 °C, 100 °C, and 160 °C, respectively. These product ion formation pathway trees for YGGFL indicate that the increased abundances of lower mass-to-charge product ions in the elevated temperature spectra result from an increase of both the consecutive dissociation and competitive dissociation pathways. For example, in Scheme 2, when the temperature is elevated to 100 °C, most of the b_3 product ion is formed from the second- and third-stage dissociation pathways (consecutive dissociation) while much less of b_3 is formed from the first-generation competitive dissociation pathway. However, the relative amount of the b_3 dissociation pathway increases with increasing temperature, indicating that is becoming a more competitive pathway too. Conversely, when the temperature is further elevated to 160 °C and more of the b_3 product ion is formed from the competitive dissociation of the parent ion its formation becomes less competitive in the second- and third-stage dissociation.

It is not surprising that elevated temperatures result in increased consecutive dissociation pathways. When the temperature is elevated, parent ions initially have more internal energy and thus can be activated to a higher total energy. Thus, assuming statistical partitioning of the excess internal energy to the dissociation products, the product ions will have more internal energy and can subsequently undergo more consecutive dissociation. For instance, when the temperature is raised to 100 °C, the relative abundance of the second- and third-stage b_3 product ion formation pathways increase as shown in Scheme 2. When the temperature is further raised to 160 °C, the a_4 competitive dissociation pathway

Table 2
Relative abundances of the major FLLVPLG product ions at different temperatures.

Temperature (°C)	Product ion						
	b_6	b_4	a_4	*m/z* 428	b_3	*m/z* 329	*m/z* 315
30	6.1	70.2	13.7	1.1	6.0	1.9	1.0
100	6.3	66.5	15.2	1.4	5.6	3.5	1.4
160	6.9	54.0	17.9	3.3	10.3	5.5	2.2

of the $[M+H]^+$ pathway disappears and the entire a_4 product ion is formed from the consecutive dissociation of the b_4 ion. This further supports the assumption that the first-generation a_4 ions formed at ambient and 100 °C are formed by direct dissociation and not consecutively from the b_4 before it can be ejected in the double resonance experiment. If the $b_4 \rightarrow a_4$ pathway was a fast consecutive dissociation, that pathway should increase with increasing internal energy.

The loss of the direct dissociation to a_4 results in a relative increase in the formation of *m/z* 323 and *m/z* 295 as third-stage product ions, but their relative abundance in the MS/MS spectrum is unchanged as this was the dominant pathway to begin with. The relative abundance of third-stage *m/z* 380 product ions that are formed also increases when the temperature is raised from 100 °C to 160 °C. Although the a_4 consecutive dissociation pathway increases at 160 °C, the formation of b_3 by consecutive dissociation pathways decreases significantly, leading to an overall decreased abundance of the b_3 ion at 160 °C as illustrated in Table 1. At this temperature the b_4 to a_4 dissociation pathway becomes more favored relative to the other second-stage product ions. Also, it has been previously suggested that the rearrangement ions, *m/z* 323 and *m/z* 295, become more competitive with the b_3 product ion when the experimental time frame is increased and this is observed here [36]. In fact the one consistent trend in going to higher temperature is the increase in rearrangement product ions.

As a comparison to YGGFL, a larger peptide, FLLVPLG was studied. YGGFL does not have any residues that are known to have a significant affect on dissociation, but still there is one pathway that over 90% of the product ions go through ($[M+H]^+ \rightarrow b_4$). FLLVPLG does have a residue known to influence dissociation, proline [23,25] and dissociation directed by the proline should give a b_4 ion.

There are many similarities between the behavior of YGGFL and FLLVPLG. Table 2 is a tabulation of the MS/MS spectra of FLLVPLG at the three temperatures used in this study. The dissociation pathway trees and product ion formation trees are shown

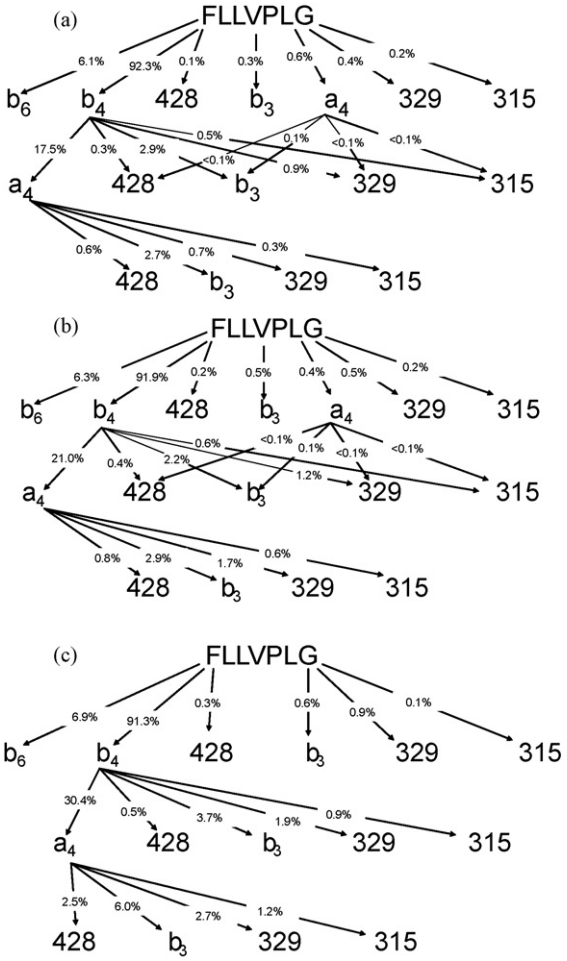

Scheme 3. Dissociation pathway trees depicting the dissociation pathways of FLLVPLG. Next to each arrow is a number displaying the abundance of that dissociation pathway. (a) 30 °C, (b) 100 °C, and (c) 160 °C.

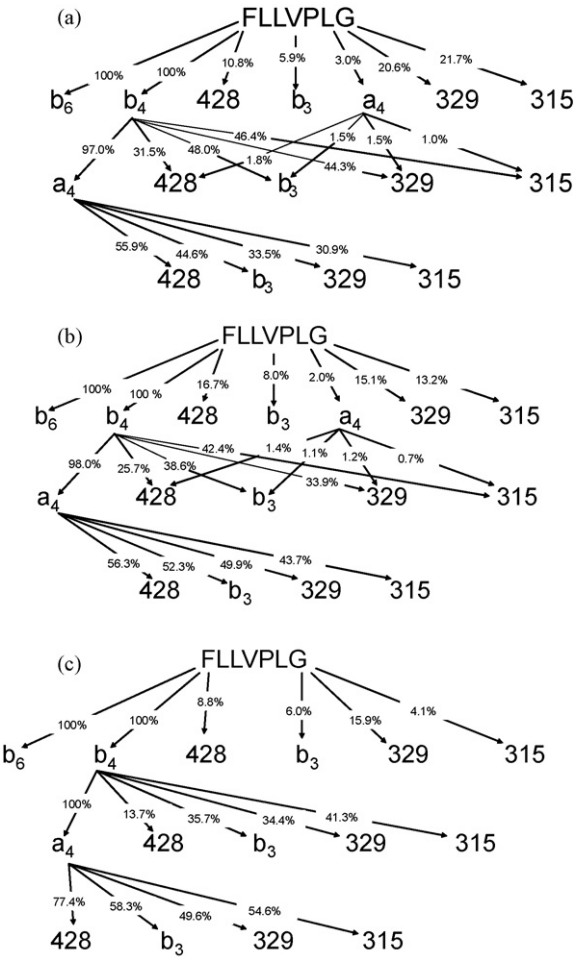

Scheme 4. Product ion formation pathway trees for FLLVPLG. Next to each arrow is the relative abundance of that that pathway contributing to the formation of that particular product ion. (a) 30 °C, (b) 100 °C, and (c) 160 °C.

in Schemes 3 and 4. Like YGGFL, greater than 90% of the dissociation of the $[M+H]^+$ goes through the b_4 pathway for FLLPVLG (Scheme 3). Also like YGGFL, the predominant dissociation pathway of b_4 is the formation of a_4. However, $b_4 \rightarrow a_4$ pathway occurs to a much smaller extent for FLLVPLG than YGGF, less than half as probable at all temperatures studied. This may be due to the fact that the neutral fragment is larger for the larger peptide and thus more of the excess internal energy is partitioned into the neutral, and thus less in the product ion, which reduces the consecutive fragmentation.

Also analogous to YGGFL, an ion corresponding to a_4-17 (m/z 428) is formed directly from $[M+H]^+$, as a second-stage product through b_4, and a third-stage product through a_4. There is also a corresponding rearrangement ion observed at m/z 315. Interestingly, there is an ion corresponding to a_3-17 (m/z 329), but no a_3. As noted before, b_3 ions generally do not dissociate to a_3, so it is not known if m/z 329 is actually a_3-17 or some kind of rearrangement ion. Again, like YGGFL, the b_3 ion appears to be a terminal ion. Another similarity between these two peptides is that the formation of a_4 directly from $[M+H]^+$ disappears at 160 °C.

For FLLVPLG the abundance of the lower mass-to-charge product ions increases with temperature. The b_6 product ion is also observed for FLLVPLG. Because FLLVPLG has two more residues than YGGFL, the b_6 ion might be considered analogous to the b_4 from YGGFL as both result from loss of the C-terminal residue. However, double resonance experiments indicate that b_6 does not consecutively dissociate after it is formed. This is most likely due to constraints imposed by the proline in the fifth position of FLLVPLG. The loss of a leucine from the b_6 product ion to form a b_5 product ion is unfavorable because proline does not allow the oxazolone structure to be formed [9]. Thus $b_6 \rightarrow b_5$ is probably a high-energy process. However, it is surprising that no a_6 ion is observed.

Overall the consecutive dissociation pathways in FLLVPLG increase with temperature, as would be expected. However, there is little change in the relative amount of the competitive dissociation pathways.

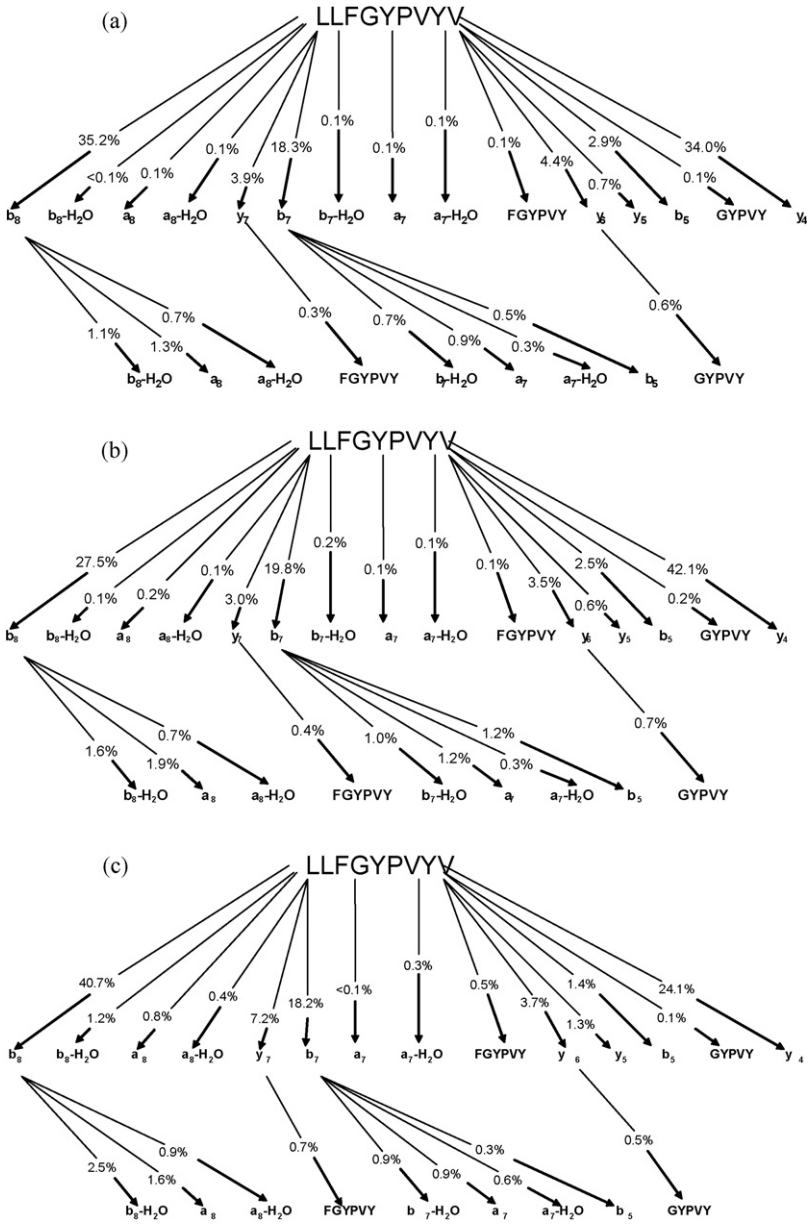

Scheme 5. Dissociation pathway trees depicting the dissociation pathways of LLFGYPVYV. Next to each arrow is a number displaying the abundance of that dissociation pathway. (a) 30 °C, (b) 100 °C, and (c) 160 °C.

Table 3
Relative abundances of the major LLFGYPVYV product ions at different temperatures.

Temperature (°C)	Product ion									
	b_8	a_8	y_7	b_7	a_7	FGYPVY	y_6	b_5	GYPVY	y_4
30	33.1	1.5	3.7	16.5	1.1	0.4	3.9	3.5	0.7	35.3
100	24.5	2.2	2.7	16.8	1.4	0.5	2.8	3.9	1.0	44.1
160	38.8	2.7	7.1	16.8	1.0	1.3	3.5	2.0	0.7	26.4

To further compare different peptide dissociation pathways, experiments were performed using the peptide, LLFGYPVYV. This peptide also has a proline which directs the dissociation, but is different than FLLVPLG in that significant y ions are observed. Table 3 is a tabulation of the MS/MS spectra of LLFGYPVYV at the three temperatures used in this study. The dissociation pathway trees and product ion formation trees are shown in Schemes 5 and 6. As can be seen in Schemes 5 and 6, there are many more competitive dissociation pathways from the $[M+H]^+$ and limited consecutive dissociation. The b-type product ions do not dissociate very readily into lower b-type product ions. The b_n product ions for this peptide appear, instead, to readily lose water (presumably due to the presence of tyrosines) and to dissociate to their corresponding a_n product ions. This is also evidenced in the MS^3 spectra (not shown). For instance, the b_8 product ion mainly dissociates to the b_8-H_2O, a_8, and a_8-H_2O product ions. Likewise the b_7 product ion dissociates to the b_7-H_2O, a_7, and a_7-H_2O product ions. Again, as with FLLVPLG, the proline probably prevents formation of the b_6 ion. However, the proline residue can be skipped as evidenced by the dissociation of the b_7 product ion to the b_5 product ion.

The y-type ions in LLFGYPVYV were also ejected so that their dissociation pathways could be analyzed. Unlike the previously documented dissociation of b-type ions to lower b and a-type ions, the y-type product ions that were observed in the spectrum did

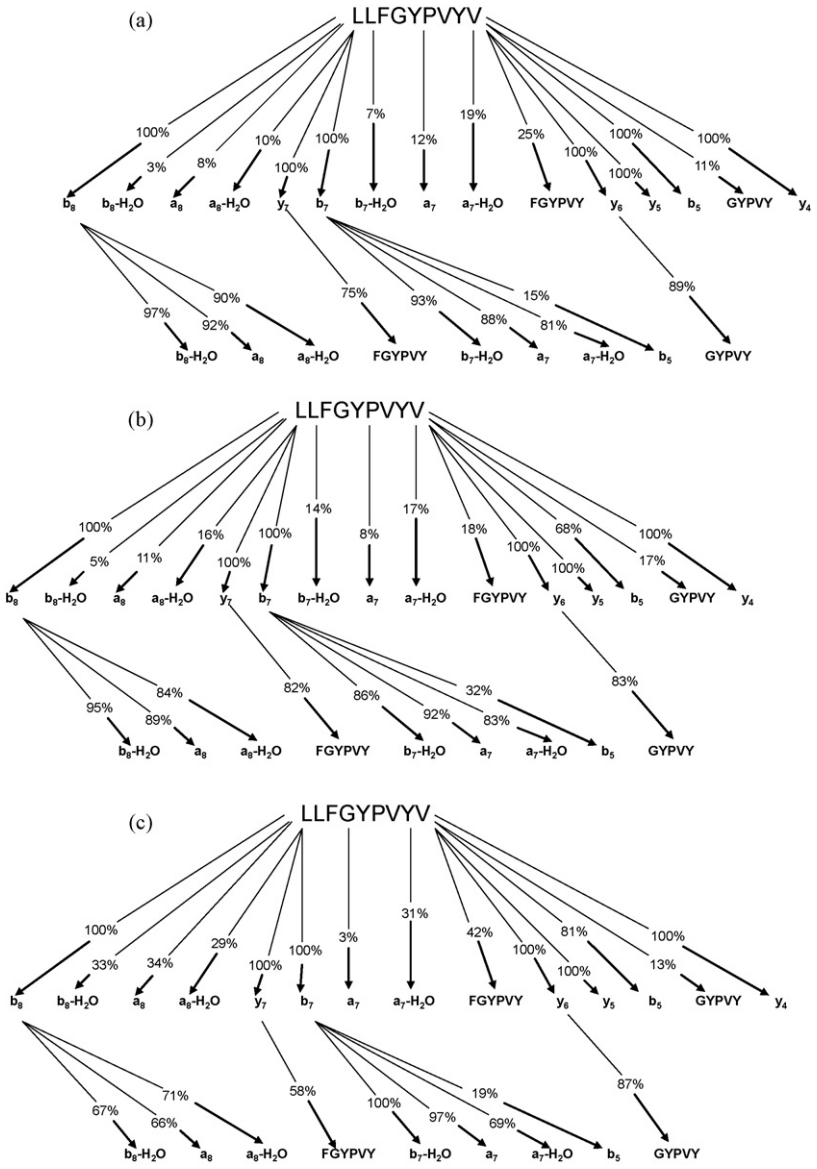

Scheme 6. Product ion formation pathway trees for LLFGYPVYV. Next to each arrow is the relative abundance of that that pathway contributing to the formation of that particular product ion. (a) 30 °C, (b) 100 °C, and (c) 160 °C.

not dissociate to lower y ions. Other groups have also observed this trend [26]. The y_7 product ion was only able to dissociate to the internal ion, FGYPVY. Likewise, the y_6 product ion was only able to dissociate to the internal ion, GYPVY. The MS^3 spectra for these two product ions (not shown) did show the y_4 product ion with reasonable intensity but this ion was not observed to be affected in the experimental double resonance spectra. The y-type ions, therefore, may preferentially dissociate to internal ions by losing the C-terminus amino acid instead of losing the N-terminus amino acid. As there were no b ions observed to consecutively dissociate by loss of the N-terminal residue(s) for any of the peptides, this suggests that "internal ions" are mainly a result of consecutive dissociation of y ions.

Competitive dissociation pathways are clearly more favored in LLFGYPVYV than they are in FLLVPLG or YGGFL. Most of the product ions show little change in relative abundance with temperature. The lack of change in relative abundance suggests that their relative rates of fragmentation do not change much as a function of internal energy. However, the two most abundant product ions, b_8 and y_4, behave differently. While b_8 initially decreases in intensity and then increases in going to the higher temperatures, y_4 is just the opposite. This could be the result of a second dissociation mechanism for the b_8 ion that becomes competitive at higher temperatures.

4. Conclusion

By performing double resonance experiments in the quadrupole ion trap the major dissociation pathways for the three peptides YGGFL, FLLVPLG, and LLFGYPVYV could be studied. For both FLLVPLG and YGGFL the vast majority of the product ions go through the same initial dissociation path, $[M+H]^+ \rightarrow b_4$. The MS/MS spectra result mainly from consecutive dissociations of N-terminal product ions. Thus, as the ion internal energy is increased (by increasing the bath gas temperature) consistent increases in the lower mass-to-charge product ion abundances are observed. This increase in lower mass-to-charge product ions is a result of the product ions having more internal energy when they are formed and therefore being more likely to dissociate to generate second- and third-stage product ions. Many of the changes in the ion abundances at different temperatures can therefore be attributed to the increased consecutive dissociation pathways. YGGFL gained access to more competitive dissociation pathways at elevated temperatures whereas FLLVPLG did not.

LLFGYPVYV did not follow the same trends as the other two peptides. It differed in that mainly C-terminal product ions were formed and instead of consecutive dissociations, competitive dissociation pathways were mainly responsible for the spectra generated. None of the first-generation product ions readily dissociated to form highly abundant second-stage product ions. Thus, increasing the ion internal energy had little affect on the MS/MS spectra. The few consecutive dissociations that were observed suggested that "internal ions" are the result of a y_n ion subsequently fragmenting at the C-terminus and not a b_n ion subsequently fragmenting at the N-terminus.

These results suggest that TA-CID in a QITMS will provide more sequence informative ions for peptides that give N-terminal containing product ions (e.g., b_n ions) although rearrangement reactions may become more prevalent. For peptides that fragment to give C-terminal containing product ions (e.g., y_n ions), TA-CID may not provide a significant increase in information.

References

[1] G.L. Glish, Multiple stage mass spectrometry: the next generation tandem mass spectrometry experiment, Analyst 119 (1994) 533–537.

[2] S.A. McLuckey, G.L. Glish, G.J.V. Berkel, Multiple stages of mass spectrometry in a quadrupole ion trap mass spectrometer: prerequisites, Int. J. Mass Spectrom. Ion Process. 106 (1991) 213–235.

[3] J.N. Louris, J.S. Brodbelt-Lustig, R.G. Cooks, G.L. Glish, G.J.V. Berkel, S.A. McLuckey, Ion isolation and sequential stages of mass spectrometry in a quadrupole ion trap mass spectrometer, Int. J. Mass Spectrom. Ion Process. 96 (2) (1990) 117–137.

[4] M.J. Charles, S.A. McLuckey, G.L. Glish, Competition between resonance ejection and ion dissociation during resonant excitation in a quadrupole ion trap, J. Am. Soc. Mass Spectrom. 5 (1994) 1031–1041.

[5] K.G. Asano, D.E. Goeringer, S.A. McLuckey, Thermal dissociation in the quadrupole ion trap: ions derived from leucine enkephalin, Int. J. Mass Spectrom. 185/186/187 (1999) 207–219.

[6] D.M. Black, A.H. Payne, G.L. Glish, Determination of cooling rates in a quadrupole ion trap, J. Am. Soc. Mass Spectrom. 17 (2006) 932–938.

[7] P.M. Remes, G.L. Glish, Collisional cooling rates in a quadrupole ion trap at sub-ambient temperatures, Int. J. Mass. Spectrom. 265 (2007) 176–181.

[8] J.V. Olsen, M. Mann, Improved peptide identification in proteomics by two consecutive stages of mass spectrometric fragmentation, PNAS 101 (37) (2004) 13417–13422.

[9] T. Yalcin, I.G. Csizmadia, M.R. Peterson, A.G. Harrison, The structure and fragmentation of B_n ($n \geq 3$) ions in peptide spectra, J. Am. Soc. Mass Spectrom. 7 (1996) 233–242.

[10] R.W. Vachet, K.L. Ray, G.L. Glish, Origin of product ions in the MS/MS spectra of peptides in a quadrupole ion trap, J. Am. Soc. Mass Spectrom. 9 (1998) 341–344.

[11] M.R. Asam, G.L. Glish, Determination of the dissociation kinetics of a transient intermediate, J. Am. Soc. Mass Spectrom. 10 (1999) 119–125.

[12] J. Laskin, T.H. Bailey, J.H. Futrell, Mechanisms of peptide fragmentation from time- and energy-resolved surface-induced dissociation studies: dissociation of angiotensin analogs, Int. J. Mass Spectrom. 249 (2006) 462–472.

[13] D.O. Konn, J. Murrell, D. Despeyroux, S.J. Gaskell, Comparison of the effects of ionization mechanism. Analyte concentration, and ion "Cool-Times" on the internal energies of peptide ions produced by electrospray and atmospheric pressure matrix-assisted laser desorption ionization, J. Am. Soc. Mass Spectrom. 16 (2005) 743–751.

[14] V.H. Wysocki, K.A. Resing, Q.F. Zhang, G.L. Cheng, Mass spectrometry of peptides and proteins, Methods 35 (3) (2005) 211–222.

[15] S.-W. Lee, H.S. Kim, J.L. Beauchamp, Salt bridge chemistry applied to gas-phase peptide sequencing: selective fragmentation of sodiated gas-phase peptide ions adjacent to aspartic acid residues, J. Am. Chem. Soc. 120 (1998) 3188–3195.

[16] T. Lin, G.L. Glish, C-terminal peptide sequencing via multistage mass spectrometry, Anal. Chem. 70 (24) (1998) 5162–5165.

[17] B. Paizs, S. Suhai, Fragmentation pathways of protonated peptides, Mass Spectrom. Rev. 24 (4) (2005) 508–548.

[18] A.R. Dongre, J.L. Jones, A. Somogyi, V.H. Wysocki, Influence of peptide composition, gas-phase basicity, and chemical modification on fragmentation efficiency: evidence for the mobile proton model, J. Am. Chem. Soc. 118 (35) (1996) 8365–8374.

[19] J. Qin, B.T. Chait, Preferential fragmentation of protonated gas-phase peptide ions adjacent to acidic amino acid residues, J. Am. Chem. Soc. 117 (1995) 5411–5412.

[20] T.H. Bailey, J. Laskin, J.H. Futrell, Energetics of selective cleavage at acidic residues studied by time- and energy-resolved surface-induced dissociation in FT-ICR MS, Int. J. Mass Spectrom. 222 (1–3) (2003) 313–327.

[21] Y.Y. Huang, V.H. Wysocki, D.L. Tabb, J.R. Yates, The influence of histidine on cleavage C-terminal to acidic residues in doubly protonated tryptic peptides, Int. J. Mass Spectrom. 219 (1) (2002) 233–244.

[22] A.G. Harrison, A.B. Young, Fragmentation reactions of deprotonated peptides containing proline. The proline effect, J. Mass Spectrom. 40 (9) (2005) 1173–1186.

[23] T. Vaisar, J. Urban, Probing the proline effect in CID of protonated peptides, J. Mass Spectrom. 31 (1996) 1185–1187.

[24] J.A. Loo, C.G. Edmonds, R.D. Smith, Tandem mass spectrometry of very large molecules. 2. Dissociation of multiply charged proline-containing proteins from electrospray ionization, Anal. Chem. 65 (1993) 425–438.

[25] B.L. Schwartz, M.M. Bursey, Some proline substituent effects in the tandem mass spectrum of protonated pentaalanine, Biol. Mass Spectrom. 21 (1992) 92–96.

[26] V.S. Rakov, O.V. Borisov, C.M. Whitehouse, Establishing low-energy sequential decomposition pathways of leucine enkephalin and its N- and C-terminus fragments using multiple-resonance CID in quadrupolar ion guide, J. Am. Soc. Mass Spectrom. 15 (12) (2004) 1794–1809.

[27] Z. Zhang, Prediction of low-energy collision-induced dissociation spectra of peptides, Anal. Chem. 76 (14) (2004) 3908–3922.

[28] M.L. Bandu, J. Wilson, R.W. Vachet, D.S. Dalpathado, H. Desaire, STEP (Statistical Test of Equivalent Pathways) analysis: a mass spectrometric method for carbohydrates and peptides, Anal. Chem. 77 (18) (2005) 5886–5893.

[29] V.M. Doroshenko, R.J. Cotter, Pulsed gas introduction for increasing peptide CID efficiency in a MALDI/quadrupole ion trap mass spectrometer, Anal. Chem. 68 (1996) 463–472.

[30] R.W. Vachet, G.L. Glish, Effects of heavy gases on the tandem mass spectra of peptide ions in the quadrupole ion trap, J. Am. Soc. Mass Spectrom. 7 (1996) 1194–1202.

[31] K.G. Asano, D.E. Goeringer, D.J. Butcher, S.A. McLuckey, Bath gas temperature and the appearance of ion trap tandem mass spectra of high-mass ions, Int. J. Mass Spectrom. 190/191 (1999) 281–293.

[32] D.E. Goeringer, K.G. Asano, S.A. McLuckey, Ion internal temperature and ion trap collisional activation: protonated leucine enkephalin, Int. J. Mass Spectrom. 182/183 (1999) 275–288.
[33] G.C.J. Stafford, P.E. Kelley, J.E.P. Syka, W.E. Reynolds, J.F.J. Todd, Recent improvements in and analytical applications of advanced ion trap technology, Int. J. Mass Spectrom. Ion Process. 60 (1984) 85–98.
[34] A.H. Payne, G.L. Glish, Thermally assisted infrared multiphoton photodissociation in a quadrupole ion trap, Anal. Chem. 73 (2001) 3542–3548.
[35] A.H. Racine, A.H. Payne, P.M. Remes, G.L. Glish, Thermally assisted collision-induced dissociation in a quadrupole ion trap mass spectrometer, Anal. Chem. 78 (13) (2006) 4609–4614.
[36] R.W. Vachet, B.M. Bishop, B.W. Erickson, G.L. Glish, Novel peptide dissociation: gas-phase intramolecular rearrangement of internal amino acid residues, J. Am. Chem. Soc. 119 (24) (1997) 5481–5488.
[37] P. Thibault, A.J. Alexander, R.K. Boyd, K.B. Tomer, Delayed dissociation spectra of survivor ions from high-energy collisional activation, J. Am. Soc. Mass Spectrom. 4 (1993) 845–854.
[38] J.M. Allen, A.H. Racine, A.M. Berman, J.S. Johnson, B.J. Bythell, B. Paizs, G.L. Glish, Why are a_3 ions rarely observed? J. Am. Soc. Mass Spectrom. 19 (2008) 1764–1770.